Scaling investigation of natural convection heat transfer and fluid flow of low Prandtl fluids over a heated vertical wall

Matthew N. Ottah, Olayinka O. Adewumi and Ayowole A. Oyediran
[1]Department of Mechanical Engineering, University of Lagos, Lagos, Nigeria
E-mail: oadewunmi@unilag.edu.ng; ayooyediran@hotmail.com

Abstract

This work presents numerical analysis for two-dimensional laminar free convection over a vertical isothermal and constant heat flux wall of low Prandtl number Newtonian fluids. The Bejan's method of scale analysis is used to obtain the governing partial differential equations while similarity transformation is employed to transform the partial differential equations to ordinary differential equations. Bejan's method of scale analysis shows the influence of balance of forces that affects the boundary layer flow and heat transfer. In this study, results show that Grashof number is the relevant dimensionless group describing the flow as against Raleigh number which was used to generalize the flow for both inner and outer layer other researchers. The velocity layer which is the inner layer closest to the solid wall dominated by the friction – buoyancy force balance is considered in this study. The governing equations are solved using the classical fourth order Runge – Kutta numerical method coupled with shooting method; multi-step differential transformation method and Keller box method and results obtained are compared. Results for velocity, temperature, local Nusselt number and skin friction were obtained for Prandtl numbers of 0.001, 0.01, 0.1, 0.5, and 0.72. The scales derived for low Prandtl flows in this study show that Grashof number is only applicable to the velocity boundary layer for low Prandtl flows. Results obtained were compared to those reported in open literature and there was 29% difference in the values obtained for local skin friction while the results for Nusselt number there was a difference factor of $Pr^{1/2}$.

Keywords: *Newtonian fluid, Grashof number, Prandtl number, Scale analysis, boundary layer*

1.0 INTRODUCTION

In natural convection flows, fluid undergoes motion as a result of temperature difference which creates a density difference within the fluid. The warmer fluid, which is less dense than unheated fluid rises relative to the cooler fluid. The flow may be external, in which case the wall is located in an infinite system of ambient fluid, or internal, in which case the wall may be heated, cooled or insulated. The study of natural convection of low Prandtl fluids over a vertical wall has attracted the interest of many investigators. In view of its application in the industries such as design of solar reflectors, thermo-clinical equipment, heating and cooling emanating from nuclear reactors, oven design etc., considerable efforts have been made to understand the heat transfer and flow of low Prandtl fluids over heated walls. Such study can be seen in the classic work by Eckert [1] adopting the method of Karman – Pohlhausen, Ostrach [2] and Kuiken [3] who referenced Lefevre's asymptotic solution for low Prandtl flows. Experimental [9-11] and numerical [12-25] investigations have also been carried out by different researchers for high Prandtl numbers natural convection flows over a heated vertical plate for both Newtonian and non-Newtonian fluids [3, 7, 14-18].

Experimental information on natural convection in low Prandtl fluid is unfolding at a slow rate [8] and this shows that developing experimental models for heat transfer studies of low Prandtl fluids is a major challenge in the field. Previous studies are limited to Prandtl number of 0.003 because at lower Prandtl number, computation codes started breaking down. An equally important wall model is the uniform heat flux condition. In many applications, the wall heating effect is the result of radiation heating from the other side or, as in the case of electronic components, the result of resistive heating. The constant heat flux condition

applies to nuclear radiation heating under special conditions. Recent works using Bejan's scaling method can been seen in [5, 21, 23, and 26] for high Prandtl numbers for vertical heated plate. Bejan [23] used scale analysis to obtain scaling laws for the dominant parameters in boundary layer flows and heat transfer. In the study carried out by Bejan and Khair, results obtained using these scaling laws was in agreement with the exact solutions of Shapiro and Fedorovich [26] for High Prandtl numbers. For the low Prandtl numbers, inappropriate momentum equation was used for low Prandtl numbers [21] and as a result, it is the aim of this study to present the appropriate Bejan's scaling laws and appropriate dimensionless group for Low Prandtl numbers and the transformed equations along with the boundary conditions are solved numerically [23, 25] for the local Nusselt numbers, local skin friction, velocity and temperature distributions for low Prandtl numbers. Scaling analysis shows that Grashof number is only applicable in the velocity boundary region in the range of Prandtl numbers less than 1 while most researchers have been using this dimensionless number for all low and high Prandtl numbers velocity and thermal boundary layers.

2.0 PHYSICAL MODEL, GOVERNING EQUATIONS AND BOUNDARY CONDITIONS

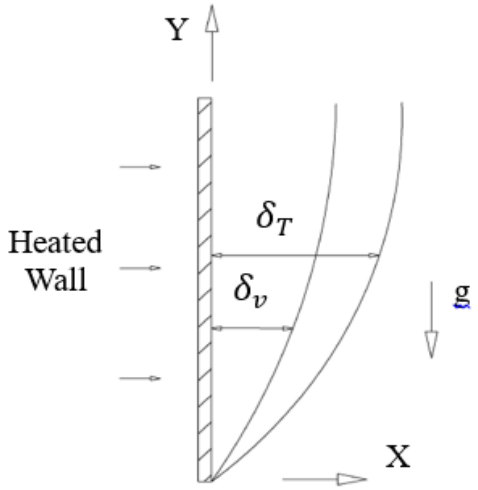

Figure 1: Boundary layer over a heated vertical wall for low Prandtl fluids

Consider a steady, two-dimensional boundary layer flow of an incompressible Newtonian fluid over a hot semi – finite vertical wall situated in a quiescent bulk of fluid as shown in Figure 1. The wall has either a uniform surface temperature (UST) or uniform heat flux (UHF) boundary condition. Applying boundary layer model and Boussinesq approximations, the governing equations for convective, laminar and steady flow can written be as;

$$\frac{\partial u}{\partial x}+\frac{\partial v}{\partial y}=0 \quad (1)$$

$$u\frac{\partial v}{\partial x} + v\frac{\partial v}{\partial y} = \upsilon\frac{\partial^2 v}{\partial x^2} + g\beta(T - T_\infty) \quad (2)$$

$$u\frac{\partial T}{\partial x} + v\frac{\partial T}{\partial y} = \alpha\frac{\partial^2 T}{\partial x^2} \quad (3)$$

The associated boundary conditions are; at $x = 0; u = v = 0, T = T_0(\text{UST})$;
$-k\frac{\partial T}{\partial x} = q_w(\text{UHF})$; as $x \to \infty;\ u \to 0, T \to T_\infty$.

Also, at $y = 0; u = 0, T = T_0$.
Using Bejan's method of scale analysis [23], where $x \sim \delta_v$, $y \sim h$, $\delta_v << H$, the boundary layer equations (1) to (3) scale as;

$$\frac{u}{\delta_v} \approx \frac{v}{H} \quad (4)$$

$$u\frac{v}{\delta_v}, v\frac{v}{H} \approx \upsilon\frac{v}{\delta_v^2}, g\beta\Delta T \quad (5)$$

$$u\frac{\Delta T}{\delta_v}, v\frac{\Delta T}{H} \approx \alpha\frac{\Delta T}{\delta_v^2} \quad (6)$$

From equation (6), we obtain the velocity scale as

$$v \approx \frac{\alpha H}{\delta_v^2} \quad (7)$$

Equations (4) to (6) gives us the balance between friction and buoyancy forces in the velocity boundary layer of thickness δ_v. Substituting the expression in equation (7) into equation (5) we obtain the scales for the velocity boundary layer δ_v shown in equation (8).

$$\delta_v(y) = \begin{cases} yGr_y^{-1/4} \text{ For UST case} \\ yGr_y^{-1/5} \text{ For UHF case} \end{cases}$$

Where, $Gr_y = \frac{g\beta\Delta T}{\upsilon^2}y^3, Gr_{*y} = \frac{g\beta q"}{\upsilon^2 k}y^4, Ra_{*y} = \frac{g\beta q"}{\alpha\upsilon k}y^4, \text{Pr} = \frac{\upsilon}{\alpha}, Bo_y = \frac{g\beta\Delta T}{\alpha\upsilon}y^3\text{Pr}$
The dimensionless variables are,

$$\eta = \frac{x}{\delta_v(y)}$$

$$\theta(\eta) = \begin{cases} \dfrac{T - T_\infty}{T_0 - T_\infty} \text{ for UST case} \\ \dfrac{T - T_\infty}{\frac{q_0 \delta_v(y)}{k}} \text{ for UHF case} \end{cases} \quad (10)$$

$$\psi(\eta) = \begin{cases} \alpha Ra_y{}^{1/4} \Pr^{\frac{3}{4}} f(\eta) & \text{for UST case} \\ \alpha C \Pr y^{\frac{4}{5}} f(\eta) & \text{for UHF case} \end{cases} \quad (11)$$

Where $C = \left(\frac{g\beta q''}{\alpha \nu k} . \frac{1}{\Pr}\right)^{-1/5}$

The stream function $\psi(\eta)$ satisfies the continuity equation by $u = \frac{\partial \psi}{\partial y}$; $v = -\frac{\partial \psi}{\partial x}$

The partial differential equations (2) and (3) are transformed into ordinary differential equations (12) and (13) using similarity formulation.

$$mf'^2 + nff'' = -f''' + \theta \quad (12)$$

$$-\Pr\left[nf\theta' + A\left(\frac{4}{5} - m\right)f'\theta\right] = \theta'' \quad (13)$$

The boundary conditions are

$$f(0) = f'(0) = 0,\ \theta(0) = 1 \text{ or } \theta'(0) = -1 \qquad f'(\infty) \to 0,\ \theta(\infty) \to 0 \quad (14)$$

Where $A = \begin{cases} 0 \text{ for UST case} \\ 1 \text{ for UHF case} \end{cases}$, $m = \begin{cases} 1/2 \text{ for UST case} \\ 3/5 \text{ for UHF case} \end{cases}$, $n = \begin{cases} -3/4 \text{ for UST case} \\ -4/5 \text{ for UHF case} \end{cases}$

The wall shear stress and local skin friction coefficient are given by equations (15) and (16) respectively.

$$\tau_w = \begin{cases} \dfrac{-\mu\alpha}{y^2} Gr_y{}^{3/4} f''(0) \text{for UST case} \\ \dfrac{-\mu\alpha}{y^2} Gr_{*y}{}^{3/5} \Pr f"(0) \text{ for UHF case} \end{cases} \quad (15)$$

$$C_{f,y} = \begin{cases} \dfrac{\tau_w}{\left(\frac{\mu\alpha}{y^2} Gr_y{}^{\frac{3}{4}}\right)} \text{for UST case} \\ \dfrac{\tau_w}{\frac{\mu\alpha}{y^2} Gr_{*\mathrm{y}}{}^{\frac{3}{5}} \Pr} \text{for UHF case} \end{cases} \quad (16)$$

The local heat transfer coefficient and Nusselt number are given by equations (17) and (18) respectively.

$$h = \begin{cases} -\theta'(0) \frac{k}{\mathrm{y}} Gr_y{}^{\frac{1}{4}} \text{ for UST case} \\ \frac{1}{\theta'(0)} \frac{k}{y} Gr_{*y}{}^{1/5} \text{ for UHF case} \end{cases} \quad (17)$$

$$\begin{cases} \dfrac{Nu_y}{\mathrm{Gr_y}^{1/4}} = -\theta'(0) & \text{for UST case} \\ \dfrac{Nu_y}{\mathrm{Gr_{*y}}^{1/5}} = \dfrac{1}{\theta'(0)} & \text{for UHF case} \end{cases} \tag{18}$$

Table 1 shows a comparison between the scales used by Kuiken [3] in his work and those used in this study obtained using Bejan's scale analysis [23].

2.1 METHOD OF SOLUTION

The system of coupled, non-linear ordinary differential equations (12) and (13) are solved first by converting it to a system of first order ODEs such that;

$$\begin{aligned} z_1 &= \theta \\ z_2 = z_1{}' &= \theta' \\ z_3 &= f \\ z_4 = z_3{}' &= f' \\ z_5 = z_4{}' &= f'' \end{aligned} \tag{19}$$

We have the non-linear equations to be;

$$\begin{aligned} z_1{}' &= z_2 \\ z_2{}' &= \frac{3}{4}\mathrm{Pr} z_2 z_3 \\ z_3{}' &= z_4 \\ z_4{}' &= z_5 \\ z_5{}' &= z_1 - \frac{1}{2}z_4{}^2 + \frac{3}{4}z_3 z_5 \end{aligned} \tag{20}$$

2.1.1 Runge - Kutta method

From equation (20); Newton iteration method is computed for $f_1\left(z_1(\eta \to \infty)\right) = 0 \; and \; f_2\left(z_4(\eta \to \infty)\right) = 0;$ with a step size of η = 0.01 and shooting success criterion maximum of $[f'(\eta), \theta(\eta)] \leq 10^{-7}$ for the range of Pr numbers given were achieved and are used for the computations of the result using Runge – Kutta formulation.

2.1.2 Multi – step Differential Transformation Method (DTM)

The solution of the transformed equation (20) yields:

$$\begin{aligned} z'_1 &= z_1 + z_1(k)\eta^k \\ z'_2 &= z_2 + z_2(k)\eta^k \\ z'_3 &= z_3 + z_3(k)\eta^k \\ z'_4 &= z_4 + z_4(k)\eta^k \\ z'_5 &= z_5 + z_5(k)\eta^k \end{aligned} \tag{21}$$

Due to convergence, equation (21) solution is only valid near η = 1, thus, multi – step transformation is used. Performing differential transformation, we have the solution for $f(\eta)$ and $\theta(\eta)$ to be of the form;

$$f_i(\eta) = \sum_{i=0}^{k} (\frac{\eta}{y_i}) \bar{f}_i(k)$$
$$\theta_i(\eta) = \sum_{i=0}^{k} (\frac{\eta}{y_i}) \bar{\theta}_i(k) \quad (22)$$

Where *i, k, y_i* represents the i-th sub-domain, the number of power series and sub-domain interval respectively. $\bar{f}_i(k)$ and $\bar{\theta}_i(k)$ are transformed functions of $f_i(k)$ and $\theta_i(k)$ respectively. Equation (20) is then transformed using multi-step DTM as shown in equation (23).

$$\left.\begin{aligned} z_{1i}(k+1) &= \frac{z_2(k)}{k+1} y_i \\ z_{2i}(k+1) &= \frac{3}{4}\Pr \frac{1}{k+1} y_i \sum_{i=0}^{k} \left[\left(z_3(i) z_2(k-i) \right) \right] \\ z_{3i}(k+1) &= \frac{1}{k+1} y_i z_4(k) \\ z_{4i}(k+1) &= \frac{1}{k+1} y_i z_5(k) \\ z_{5i}(k+1) &= \frac{1}{k+1} y_i \left[z_1(k) - \frac{1}{2} \sum_{i=0}^{k} \left[\left(z_4(i) z_4(k-i) \right) \right] + \frac{3}{4} \sum_{i=0}^{k} \left[\left(z_3(i) z_5(k-i) \right) \right] \right] \end{aligned}\right\}$$

$$for\ k \in [0, y_i] \Rightarrow k \in [y_{i-1}, y_i]; \quad (23)$$

2.1.3 Keller Box method

Keller box method is used in discretizing equations (12) and (13) such that, an introduction of new independent variables were formed. Thus, we have;

$$\left.\begin{aligned} &u(x,\eta);\ v(x,\eta);\ \mathrm{t}(x,\eta);\ \theta(x,\eta) \\ &f' = u;\ u' = v;\ s' = t \end{aligned}\right\} \quad (24)$$

Equations (12) and (13) transforms to,

$$\left.\begin{aligned} v' &= \theta + \frac{3}{4} fv - \frac{u^2}{2} \\ t' &= \frac{3}{4} \Pr ft \end{aligned}\right\} \quad (25)$$

Applying finite difference scheme, centre-difference derivatives is used for the discretization of the governing equation. Equation (25) is transformed into the following;

$$f_{j-1/2} = -h_j\left(\theta + \frac{3}{4}(fv)_{j-1/2} - \frac{1}{2}(u^2)_{j-1/2} + \left(\frac{v_j - v_{j\text{-}1}}{h_j}\right)\right)$$

$$\theta_{j-1/2} = -h_j\left(\left(\frac{v_j - v_{j\text{-}1}}{h_j}\right) + \frac{3}{4}\Pr(ft)_{j-1/2}\right) \quad (26)$$

Applying Newton method of linearization for non-linear system of equation and tri-diagonal matrix, a non-singular matrix formation whose element are determined is given by the relationship;

$$[\alpha_j] = [\mathrm{A}_j] - [\mathrm{B}_j][\Gamma_{j-1}] \quad (27)$$

For i = 1, 2, 3 . . . j

$\mathrm{A}_j, \mathrm{B}_j, \Gamma_j$ are calculated using forward sweep methods and yields $\left|\delta v_o^{\,i}\right| \le \varepsilon_i$ where ε_i is a small parameter. A MATLAB code was developed for the numeric solution.

3.0 RESULTS AND DISCUSSION

Scaling investigation of natural convection of low Prandtl fluids over a heated vertical wall is analyzed and the result obtained shows the effect of Prandtl number on the temperature profile, velocity profile, local Nusselt number and local skin friction for velocity boundary layer. Tables 2 and 3 show a comparison between the different solution methods used in this study to obtain the Nusselt number and skin friction for various values of Prandtl number when the heated wall is isothermal and for constant heat flux boundary conditions. The results obtained using all the solution methods were in good agreement. This is also seen in Tables 4 and 5 which show results of temperature and velocity profiles for both isothermal and constant heat flux conditions. The method of solution adopted shows that level of accuracy of the multi-steps between intervals of 0.001 has an error of 10^{-5}.

Table 1: Scales in a velocity boundary layer along a vertical wall for low Prandtl fluids

	Kuiken[3] UST	Present study	
		UST	UHF
Similarity Variable (η)	$\frac{y}{x}\left(Gr_y \Pr^2\right)^{1/4}$	$\frac{x}{y}Gr_y^{1/4}$	$\frac{x}{y}Gr_{*y}^{1/5}$
Velocity Boundary Layer thickness, (δ_v)	$x\left(Gr_y \Pr^2\right)^{-1/4}$	$yGr_y^{-1/4}$	$yGr_{*y}^{-1/5}$
Thickness of wall jet, (δ_T)	-	$yBo_y^{-1/4}$	$yBo_{*y}^{-1/5}$
Velocity scale, v	$\frac{\alpha}{x}Gr_y^{1/2}\Pr^2$	$\frac{\alpha}{y}Gr_y^{1/2}\Pr$	$\frac{\alpha}{y}Gr_{*y}^{2/5}\Pr$
Local Nusselt number	$Nu/\left(Gr_y \Pr^2\right)^{1/4} = 0.60040 - 0.32385\Pr^{1/2}$	$Gr_y^{1/4}$	$Gr_{*y}^{1/5}$

Local Skin friction	$\left.\frac{d^2 f}{dn^2}\right\|_{\eta=0} = 1.0699496 - 1.001023\,\mathrm{Pr}^{1/2}$	$\tau_w / \left(\frac{\mu\alpha}{y^2} Gr_y^{3/4}\,\mathrm{Pr}\right)$	$\tau_w / \left(\frac{\mu\alpha}{y^2} Gr_{*y}^{3/5}\,\mathrm{Pr}\right)$

Table 2: Comparison of the methods of solution for isothermal condition

Pr	Case	$\theta'(0)$			$f''(0)$		
		RK4	DTM	Keller Box	RK4	DTM	Keller Box
0.001	UST	-0.01866978	-0.01867012	-0.01861470	-1.47288745	-1.46986940	-1.46986785
0.01		-0.05698121	-0.05698245	-0.05698457	-1.39699878	-1.38658213	-1.38658774
0.1		-0.16274635	-0.16274956	-0.16274568	-1.21512154	-1.20959531	-1.20959221
0.5		-0.31195451	-0.31196001	-0.31196254	-1.00863254	-1.00074236	-1.00074632
0.72		-0.35683121	-0.35684101	-0.35684459	-0.95604012	-0.95589969	-0.95589415

Table 3: Comparison of the methods of solution for uniform heat flux condition

Pr	Case	$1/\theta'(0)$			$f''(0)$		
		RK4	DTM	KELLER BOX	RK4	DTM	KELLER BOX
0.001	UHF	0.04727241	0.04725451	0.04725478	13.7483658	-13.7247201	-13.7245658
0.01		0.11496525	0.11477941	0.11477256	6.70013261	-6.68975560	-6.68975648
0.1		0.26348368	0.26230943	0.26230458	3.12854853	-3.12731523	-3.12738987
0.5		0.43892747	0.43830833	0.43830621	1.76999884	-1.75148896	-1.75146897
0.72		0.48730799	0.48546815	0.48546777	1.55032451	-1.52157482	-1.52157380

The difference between the results obtained in this study using scale analysis and those obtained by Kuiken [3] was a factor of $Pr^{1/2}$.This is due to the fact that the dimensionless group use to describe the flow is general as in this case, Grashof number use to describe the inner layer while other researchers generalise Raleigh number for both inner and outer layer of boundary layer. Table 6 shows that if we take into consideration this factor, the results obtained using scale analysis will be similar to those of Kuiken. Results presented in Figures 2 and 3 show the temperature profiles along a heated wall for the isothermal and constant heat flux boundary conditions respectively. It can be seen that in both cases as Prandtl number decreases there is a remarkable increase in thermal thickness. As the Prandtl number decreases from 0.72 to 0.1, it approaches an asymptote rapidly than for extreme low values of Pr << 0.01. This explains why most low Prandtl number fluids have high thermal conductivity and as a result, the thermal diffusion will be an effective mode of heat transfer and this effect is applied in the design of sandwiched walls for cooling.

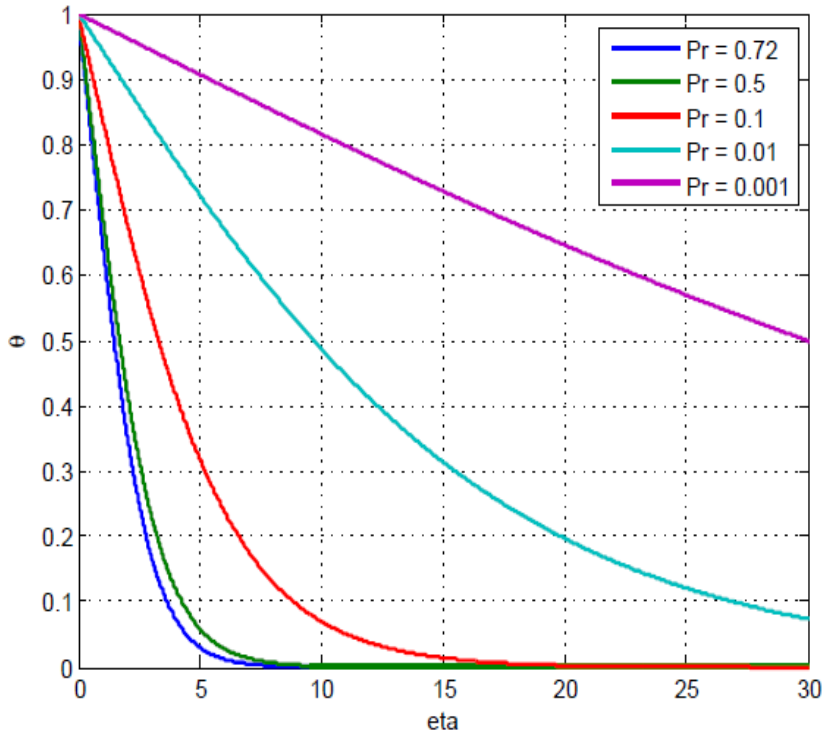

Figure 2: Effect of Prandtl number on the temperature profile for UST case

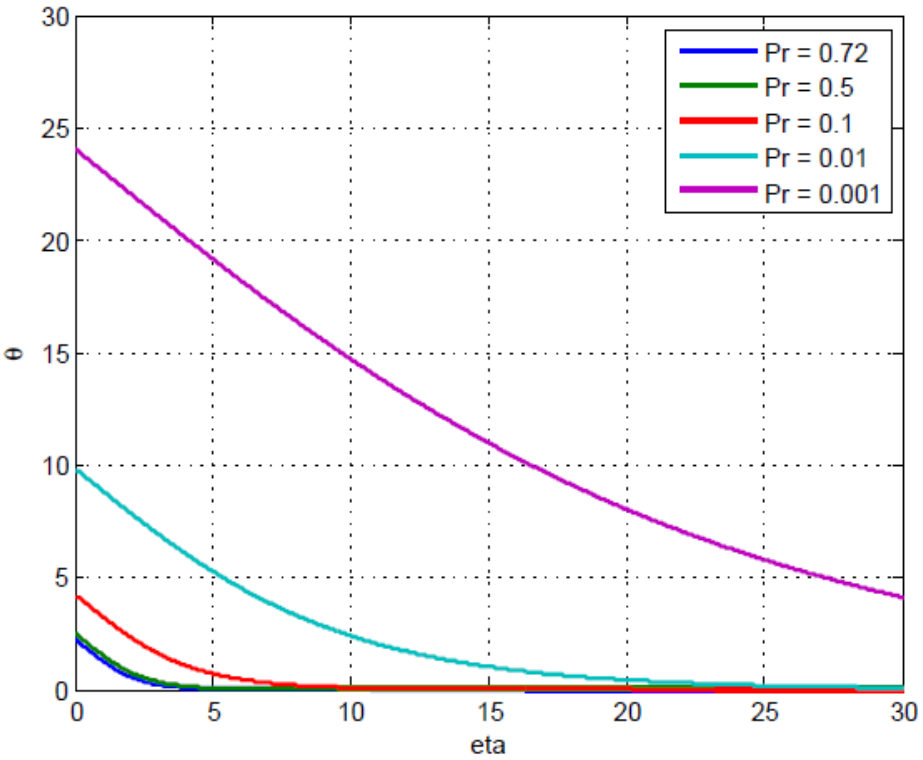

Figure 3: Effect of Prandtl number on the temperature profile for UHF case

Figures 4 and 5 show the results for dimensionless velocity and the plots show that as the Prandtl number reduces the velocity increases but approaches an asymptote. These results were compared with the scale used by Kuiken as shown in Table 1 to compute the velocities for Prandtl number of 0.003 to 0.72 for isothermal case and a difference of order of magnitude of 2 is obtained. Figure 6 shows a comparison between the convective heat transfer from a vertical wall with constant temperature and uniform heat flux respectively in terms of the local Nusselt number. The heat transfer coefficient and local Nusselt number expressions are given by equations (17) and (18). Increasing the value of Prandtl number increases the Nusselt number but a rapid rate of increase can be seen in UHF for Prandtl number$\Pr > 0.3$. This shows greater heat dissipation for the UHF case at Prandtl numbers greater than 0.3. This trend can be seen in the thermal cooling and heating designs for electrical conduction between non – metallic and metallic surfaces.

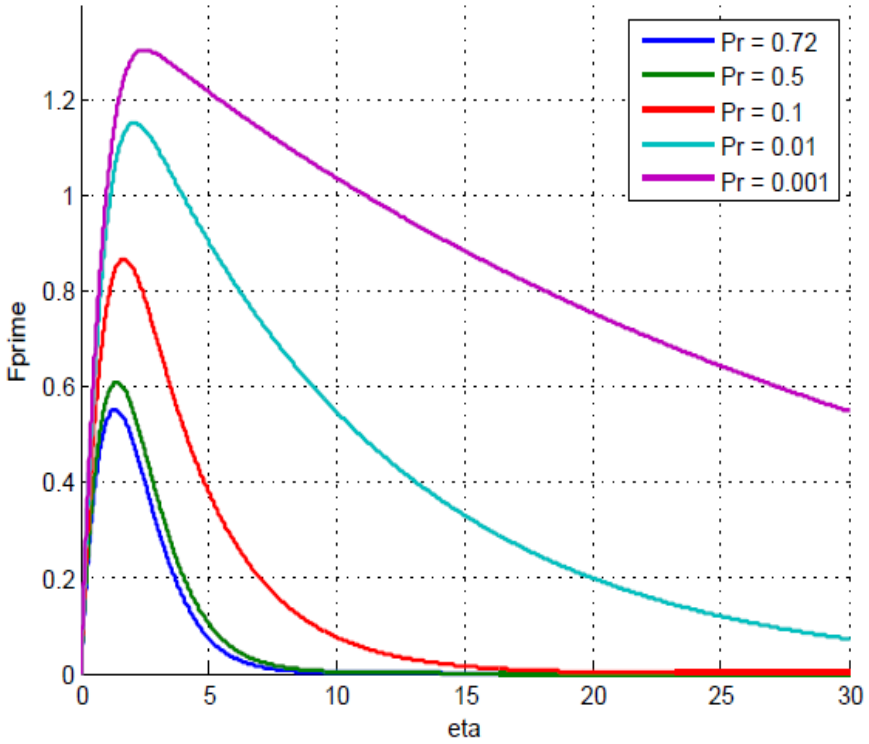

Figure 4: Effect of Prandtl number on the velocity profile for UST case

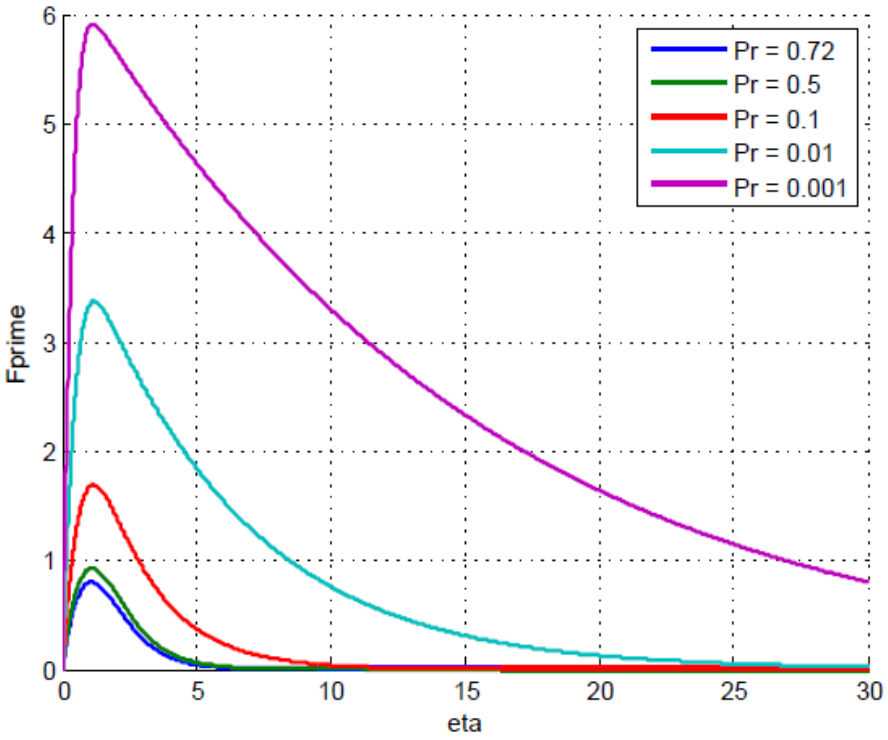

Figure 5: Effect of Prandtl number on the velocity profile for UHF case

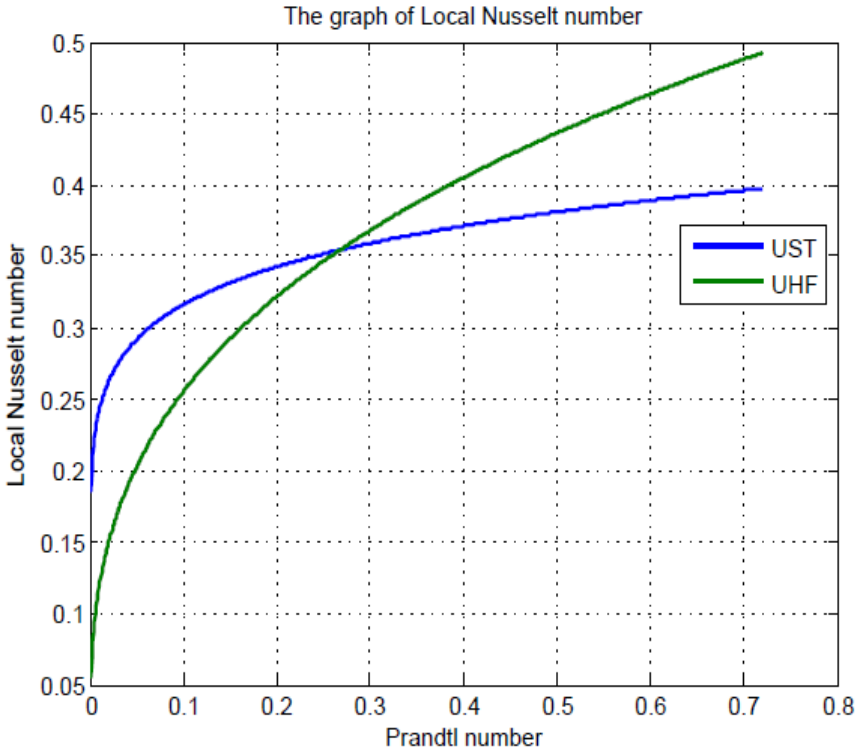

Figure 6: Comparison between local Nusselt number results for the UST and UHF cases

Figure 7 shows results of the comparison between local skin friction for the UST and UHF cases respectively. As the Prandtl number increases, the local skin friction reduces until it reaches an asymptotic value. Large values for skin friction were obtained for constant heat flux case

and this trend could be as a result of temperature non-uniformity on the heated wall. The application of the result showed is the crystallization of liquid metal cooling at extreme low temperatures in modern reactors. This result also shows that using an isothermal boundary condition leads to under prediction of the local skin friction values.

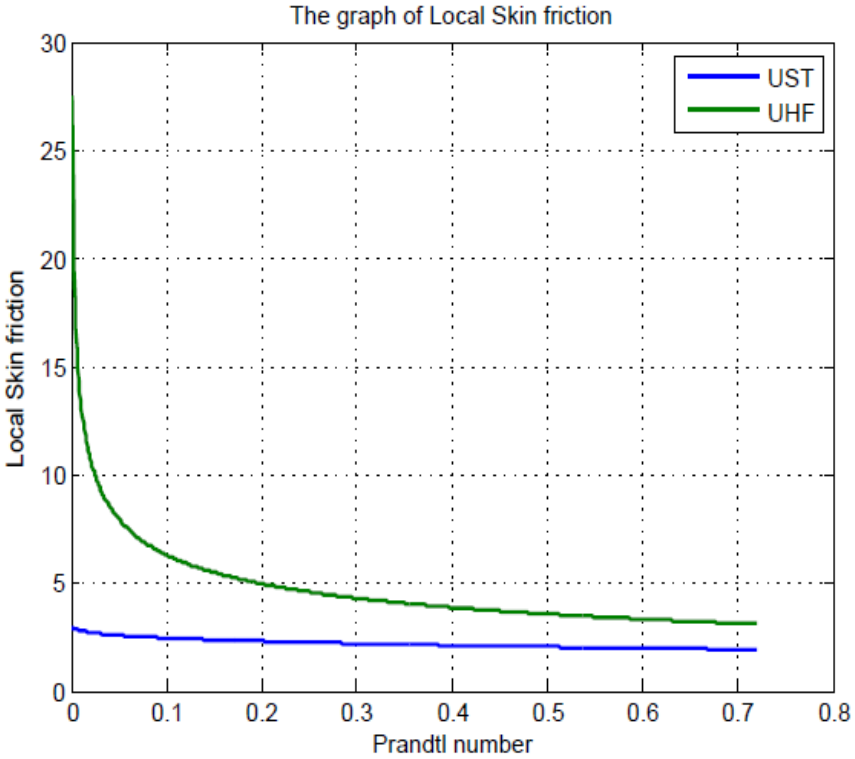

Figure 7: Comparison between local skin friction results for the UST and UHF cases

CONCLUSIONS

Scaling investigation of natural convection fluid flow of low Prandtl fluids over a heated vertical wall has been analyzed for constant temperature (USF) and constant heat flux (UHF) boundary conditions. Appropriate scaling laws obtained by Bejan's scale analysis and similarity formulation were used to transform the governing partial differentiation equations for boundary flows to ordinary differential equations. These equations were solved using three different methods of solutions for Prandtl number ranging 0.001 to 0.72. Results obtained showed that all numerical methods used in this study to solve the governing equations were in good agreement and Prandtl number has a very significant effect on the heat transfer analysis for both cases investigated in this study. The scaling method used shows clearly the interplay of forces that drive the natural convection and fluid flow within the boundary layer. The effect of Prandtl number on the temperature profile, velocity profile, local Nusselt number and skin friction are reported and results for the constant temperature and constant heat flux boundary conditions within the inner layer were also presented.

NOMENCLATURE

Bo	Boussinesq number
f	Dimensionless stream function in velocity boundary layer
F	Dimensionless stream function in temperature boundary layer
g	Acceleration due to gravity (m/s^2)
Gr_y	Grashof number

Gr_{*y}	Grashof number based on heat flux
h	Heat transfer coefficient (W/m^{2}K)
H	Height (m)
k	Thermal conductivity (W/mK)
Nu	Local Nusselt number
Pr	Prandtl number
q_w''	Heat flux at the wall (W/m^2)
Ra_y	Rayleigh number
Ra_{*y}	Rayleigh number base on heat flux
T	Temperature (K)
T_0	Wall temperature (K)
T_∞	Free stream temperature (K)
u, v	Velocity components in the x-, y-directions (m/s)
$\boldsymbol{v}$	Vertical velocity scale
x, y	Cartesian coordinates

Greek symbols

α	Thermal diffusivity (m^2/s)
β	Coefficient of thermal expansion (1/K)
δ_V	Velocity boundary layer thickness (m)
ΔT	Temperature difference (K)
η	Similarity variable
ϑ	Dimensionless temperature
ν	Kinematic viscosity (m^2/s)
ρ	Density (kg/m^3)
τ	Shear stress (N/m^2)
ψ	Stream function

Subscripts

x, y	Modified parameter
w	Wall condition
∞	Ambient condition

Superscripts

$'$	Derivative, d/dη
$*$	Uniform surface

REFERENCES

[1] Eckert, E.R.G., Drake, R.M. Jr., *Analysis of Heat and Mass Transfer*, International Student Edition, McGraw-Hill, New York, 1972.

[2] Ostrach, S., An analysis of laminar free convection flow and heat transfer about a flat plate parallel to the direction of the generating body force, *Technical Note 2635: NACA*, 1952.

[3] Kuiken, H.K., Free convection at low Prandtl numbers, *Journal of Fluid Mechanics*, Vol. 37, no. 4, pp. 785 – 793, 1969.

[4] Kwang – Tzu, Y., Edward, W.J., First order perturbations of laminar free convection boundary layers on a vertical plate, *Journal of Heat Transfer*, Vol. 86, no. 1, pp. 107 – 114, 1964.

[5] Adewumi, O.O., Adebusoye, A., Adeniyan, A., Ogbonna, N., Oyediran, A.A., Scale analysis and asymptotic solution for natural convection over a heated flat plate at high Prandtl numbers, *Proceedings of Romanian Academy, Series A: Physics, Technical Sciences, Information Science*, Vol. 19, pp. 184 – 189, 2018.

[6] Anderson, R., Bejan, A., Natural convection on both sides of a vertical wall separating fluids at different temperatures, *Journal of Heat Transfer*, Vol. 102, no. 4, pp. 630 – 635, 1980.

[7] Chen, C.H., Effect of magnetic field and suction/injection on convection heat transfer of non – Newtonian power-law fluids past a power-law stretched sheet with surface heat flux, *International Journal of Thermal Sciences*, Vol. 47, no. 7, pp. 954-961, 2008.

[8] Bejan, A., Lage, J.L., The Prandtl Number effect on the transition in Natural convection along vertical surface, *Journal of Heat Transfer*, Vol. 112, no. 3, pp. 787 – 790, 1990.

[9] Sparrow, E.M., Gregg, J.L., *Details of exact low Prandtl number boundary-layer solutions for forced and for free convection*, NASA MEMO 2-27-59, pp. 1 – 15, 1959.

[10] Brodowicz, I.L., An analysis of laminar free convection around isothermal vertical plate, *International Heat and Mass Transfer*, Vol. 11, no. 2, pp. 201 – 209, 1968.

[11] Hassan, K.E., Mohamed, S.A., Natural convection from isothermal flat surfaces, *International Journal of Heat and Mass Transfer*, Vol. 13, no. 12, pp. 1873-1886, 1970.

[12] Zariffeh, E.K., Daguenet, M., Laminar free convection on an inclined flat plate or a vertical cylinder with prescribed wall heat flux, *International Journal of Heat and Mass Transfer*, Vol. 24, no. 6, pp. 1071-1075, 1981.

[13] Martynenko, O.G., Berezovsky, A.A., Sokovishin, Y.A., Laminar free convection from a vertical plate, *International Journal of Heat and Mass Transfer*, Vol. 27, no. 6, pp. 869-881, 1984.

[14] Churchill, S.W., Transient, laminar free convection from a uniformly heated vertical plate, *Letters Heat Mass Transfer*, Vol. 2, pp. 311 -314, 1975.

[15] Kierkus, W.T., An analysis of laminar free convection flow and heat transfer about an inclined isothermal plate, *International Journal of Heat and Mass Transfer*, Vol. 11, no. 2, pp. 241-253, 1968.

[16] Oosthuizen, P.H., Paul, J.T., Natural convective heat transfer from a narrow isothermal vertical flat plate with a uniform heat flux at the surface, Proceedings of ASME-JSME Thermal Engineering Heat Transfer Summer Conference, Vancouver, British Columbia, 2007.

[17] Cianfrini, C., Corcione, M., Fontana, D.M., Laminar free convection from a vertical plate with uniform surface flux in chemically reacting system, *International Journal of Heat and Mass Transfer*, Vol. 45, no. 2, pp. 319 – 329, 2002.

[18] Kalender, A., Oosthuizen P.H., Numerical and experimental studies of natural convective heat transfer from vertical and inclined narrow isothermal flat plates, *Heat and Mass Transfer*, Vol. 47, no. 9, pp. 1181 – 1195, 2011.

[19] Khani, F., Aziz, A., Hamedi-Nezhad, S., Simultaneous heat and mass transfer in natural convection about an isothermal vertical plate, *Journal of King Saud University – Science*, Vol. 24, no. 2, pp. 123 – 129, 2012.

[20] Sparrow, E.M., Laminar free convection from a vertical plate with prescribed nonuniform wall flux or prescribed nonuniform wall temperature, *Technical Note 3508: NACA*, 1955

[21] Bachiri, M., Bouabdallah, A., An analytic investigation of the steady-state natural convection boundary layer flow on a vertical plate for a wide range of Prandtl numbers, *Heat Transfer Engineering*, Vol. 31, no. 7, pp. 608 – 616, 2010.

[22] Riley D.S., Drake D.G., Higher approximations to the free convection flow from a heated vertical flat plate, *Applied Scientific Research*, Vol. 30, no. 3, pp. 193 – 207, 1975.

[23] Bejan, A., *Convection Heat Transfer*, John Wiley & Sons, Hoboken, New Jersey, 2013.

[24] Mahajan, R.I., Gebhart, B., Higher approximations to the natural convection flow over a uniform flux vertical surface, *International Journal of Heat and Mass Transfer*, Vol. 21, no. 5, pp. 549 -556, 1978.

[25] Armfield, S.W., Patterson, J.C., Wenxian, L., Scaling investigation of the natural convection boundary layer on an evenly heated plate, *International Journal of Heat and Mass Transfer*, Vol. 50, no. 7-8, pp. 1592 – 1602, 2007.

[26] Bejan, A., Khair, K.R., Heat and mass transfer by natural convection in a porous medium, *International Journal of Heat and Mass Transfer*, Vol. 28, no. 5, pp. 909 – 918, 1985.